

## **SURFACE PROPERTIES AND THEIR CONSEQUENCES ON THE HYDROGEN SORPTION CHARACTERISTICS OF CERTAIN MATERIALS**

P. SELVAM

*Laboratory of Interdisciplinary X-ray Crystallography, University of Geneva, 24, Quai E. Ansermet, CH-1211 Geneva 4 (Switzerland) and Department of Chemistry, Indian Institute of Technology, Madras 600 036, Tamil Nadu (India)*

B. VISWANATHAN, C. S. SWAMY and V. SRINIVASAN

*Department of Chemistry, Indian Institute of Technology, Madras 600 036, Tamil Nadu (India)*

(Received December 11, 1989)

### **Summary**

Surface analyses (X-ray photoelectron spectroscopy, X-ray-induced Auger electron spectroscopy and Auger electron spectroscopy) results of some hydrogen storage intermetallic compounds of the type AB, AB<sub>5</sub>, A<sub>2</sub>B and the hydride, A<sub>2</sub>BH<sub>4</sub> (A≡Ti, La, Ca or Mg; B≡Fe, Ni or Cu) show the presence of numerous oxidation (aerial) products, such as oxides, hydroxides and carbonates. In general, the hydroxide and/or carbonate species are present in small amounts and persist only on the outer passivated surface. However, there are cases where they seem to be predominant, at least in the top few layers. Therefore such species are also expected to play an important role in the surface chemistry of the alloys and hydrides similar to that observed with surface oxides. Accordingly, the activation procedure varies for the different materials.

Upon activation the surface may be described as a supported metal system which in turn increases the activity thus explaining the rapid kinetics of the hydriding/dehydriding reactions upon cycling processes. The easy activation of certain alloys could also be explained on the basis of the reducibility and the thickness of the surface oxide layers. In other words, it could be demonstrated based on their oxidation resistance and the segregation behaviour of the metals. The specific reactivity of different systems are related to the segregation, oxidation, and reduction behaviours. Surface enrichment of iron in the TiFe system is demonstrated for the first time.

---

### **1. Introduction**

There is a growing worldwide interest in practical application of "rechargeable metal hydrides" in which either stored H<sub>2</sub> is used as fuel for both mobile and

stationary purposes or the heat of the reaction is the central element in a heat engine [1]. Research on the interaction of  $H_2$  with metals, alloys and intermetallic compounds has attracted considerable attention for reasons motivated from basic and applied points of view. For example, significant importance has been given in  $H_2$  energy technology, nuclear reactors, permanent magnets, heterogeneous catalysis, powder metallurgy, electrochemical cells and many more applications. Owing to this broad interest, these materials are studied extensively by scientists affiliated with various disciplines. Although these systems are not completely new, tremendous progress in this field could be noticed by the rapid development of the phenomenon related to the topic "metal hydrides" [2].

Among the intermetallic compounds available for  $H_2$  storage applications, the systems based on  $AB$ ,  $AB_2$ ,  $AB_5$  and  $A_2B$  have gained interest as potential materials for technological applications [1, 3]. The alloys  $LaNi_5$  and  $CaNi_5$  have received greater importance, because of their capacity to store large amounts of  $H_2$ , the ease in activation and the ability to react rapidly and reversibly at ambient temperature and moderate pressures [4]. Indeed, the alloys, such as  $TiFe$  and  $Mg_2Ni$  have been recognized as  $H_2$  carriers for transport vehicles, mainly because of their convenient pressure-composition-temperature ( $p-c-T$ ) relationships, high  $H_2$  content, favourable kinetics and the present lower cost compared with other suitable alloys [5]. However, a major problem for all these materials in technological applications is their poor resistance against poisoning by the gaseous impurities, such as  $O_2$ ,  $H_2O$  vapour,  $CO$ ,  $CO_2$  etc., present in the feed  $H_2$  gas or from atmospheric sources [6, 7]. Thus they require frequent activation treatment before they take-up  $H_2$ ; hence their surface properties and activation mechanism are very important and need to be thoroughly investigated.

Chemisorption and initial oxidation of gas molecules at the metal/alloy/hydride surface are of importance to the basic understanding of the reaction mechanisms involved. One of the fundamental questions that must be addressed is the phenomenon of "surface poisoning" or "surface deactivation". Hence the study of the surface properties with respect to "surface activation, deactivation, and reactivation" of the materials has been the focus of attention in view of the development of activation procedures as well as to improve the hydriding properties of these systems with commercial sources of  $H_2$ , namely from steam reforming of hydrocarbons, or to develop new materials which should not have the shortcomings of the other materials which are often encountered.

## 2. Passivation/deactivation

The utilization of metal hydrides for technical applications would be substantially determined by the ease with which they can be handled and their sensitivity to low purity gases. Contaminants, which are present in  $H_2$  gas or enter the system by servicing errors or by accidents or in contact with atmosphere, interact with metals, alloys, intermetallic compounds, or the hydride surface and deactivate them. That is, if the adsorption of an impurity at the surface, by either a physical or a chemical process, is greater than chemisorption of  $H_2$ , then the impurity will displace the  $H_2$

atoms thus passivating the surface [8, 9]. In other words, the impurities can interfere with the dissociation and association processes of  $H_2$  which are the most important steps of the hydriding and dehydriding reactions respectively. Thus deactivation is manifested in a decrease in the reaction rate and/or in the  $H_2$  sorption capacity with a simultaneous degradation of the parent material [6, 7].

As stated earlier, the hydriding rate is extremely sensitive to the initial cleanliness of the surface since oxidation is known to seal the surface to  $H_2$  reaction. The presence of oxide layers drastically decreases the reaction rate or even stops the reaction [10, 11]. One important surface-dependent step in the hydriding of these materials is the dissociation of the molecular hydrogen ( $H_2$ ) into atomic hydrogen (H). Many clean transition metals have the capacity of splitting the  $H_2$  molecule, but lose this property upon oxidation. Accordingly, the alloys, such as  $LaNi_5$ ,  $CaNi_5$ ,  $Mg_2Ni$ ,  $Mg_2Cu$  and  $TiFe$ , show good hydriding behaviour when they are activated. However, upon contact with air or contaminants they produce numerous oxidation products [12–19] which in turn deactivate the surface. Hence, they require periodic activation treatment [20, 21] and the activation procedures vary for the different alloys, depending upon the reducibility of the surface oxides [14].

It is also known that such surface oxide layers are produced on air-exposed hydrides [22]. The oxidized surface inhibits the release of  $H_2$ , presumably, by hindering the recombination of hydrogen atoms. In that case, the observed equilibrium pressure of the hydride is less than the expected value or the equilibrium temperatures are higher than the normal values. For example, if the hydride,  $TiFeH_2$  is cooled to liquid  $N_2$  temperature, exposed to air, and warmed back to room temperature, it is found to retain the  $H_2$  indefinitely [21]. The magnesium-based hydrides exposed to air also show an increase in the desorption temperatures [23]. Similar observations were noticed for the  $Mg-Ni$  hydrides which have been exposed to various gas atmospheres, such as air,  $N_2$ ,  $O_2$ ,  $CO$  and  $CO_2$  [24]. This corresponds to the deactivation of the surface by the adsorbed gas molecules. Hydrides of  $LaNi_5$  also show such effects towards  $SO_2$  [25]. Rather, this inevitable poisoning has been taken as an advantage in many systems to characterize the unstable compounds. Typical examples are the hydrides of  $TiFe$  and  $LaNi_5$  [21, 25].

The reaction rates and storage capacity of materials can be affected by various impurities present in the  $H_2$  gas [6, 24, 25]. Even at low concentration levels, the impurities cause severe problems in applications involving cyclic operation. By cycling, the alloy is subjected to repeated exposure to the impurity gases and damage effects accumulate.  $O_2$  and other oxygen-containing species, in particular those of moisture ( $H_2O$ ) and  $CO_2$  are of prime importance since they can originate at low levels in the  $H_2$  gas or from atmospheric sources, such as system leaks or in contact with air. It is noteworthy that the air-exposed intermetallics and hydrides always result in the formation of surface oxides and hydroxides [12–19, 22] as well as carbonates [26].

It is known that the equilibrium surface composition of most alloys often differs from their bulk composition. This means that one of the component metals of the alloy at the surface is enriched with respect to the bulk composition. This is a common feature encountered frequently and is termed as surface segregation. This

could have arisen owing to the influence of various factors on elements, namely higher  $O_2$  affinity, lower surface energy, bulk strain energy etc. [27, 28]. Thus the segregated metal gets oxidized easily and hence deactivates the surface, thereby causing unexpected effects on the properties of the materials. However, the nature of the surface structures formed, the degree of poisoning and the ease of reactivation vary markedly from alloy to alloy. Therefore it is necessary to look into these aspects carefully in order to understand the activation and deactivation mechanisms which, of course, are the basic steps in developing new materials and/or improving the existing materials.

In spite of numerous investigations on the surface properties of these materials, the aspects on which further information is desirable include the following.

(a) The reactivity and chemical state of various surface species formed before and after activation.

(b) The nature of the surface species involved in the passivation and the subsequent activation of the alloys.

(c) The cause of segregation and its role both in initial activation and cyclic deactivation processes.

(d) The identification of the actual catalytically active component for the observed sorption characteristics.

Hence, in the present study we have focused our attention to such problems and the results of X-ray photoelectron spectroscopy (XPS), X-ray-induced Auger electron spectroscopy (XAES) and Auger electron spectroscopy (AES) studies on different alloys carried out with this view in mind are the main purpose of this paper. However, this study was more extensive with individual systems [12-19, 22, 26, 29, 30] than can be presented here and only highlights and important findings will be summarized.

### 3. Materials and methods

The intermetallic compounds, TiFe, LaNi<sub>5</sub>, CaNi<sub>5</sub>, Mg<sub>2</sub>Ni, Mg<sub>2</sub>Cu and the hydride, Mg<sub>2</sub>NiH<sub>4</sub> were the same samples as have been used in our earlier investigations [15, 26, 29]. Photoelectron and Auger electron (excited both by photons and electrons) spectroscopic experiments (XPS, XAES and AES) were carried out at room temperature on as-received (as-inserted) air-exposed as well as on sputtered and  $O_2$ -treated samples. The studies were performed in an ESCALAB Mark II spectrometer (Vacuum Generator, U.K.) equipped with XPS, UPS, AES and argon ion ( $Ar^+$ ) sputtering facilities.

The XPS measurements were obtained using a Mg  $K\alpha$  radiation (10 kV, 60/100  $\mu A$ ) and a pass energy of 25/50 eV. The working pressure in the analysing chamber was maintained below  $5 \times 10^{-9}$  mbar. The samples were analysed in the air-exposed form and then subjected to  $Ar^+$  ion bombardment operated at  $5 \times 10^{-6}$  mbar pressure with a beam voltage of 8 kV and a filament current of 60/100  $\mu A$   $cm^{-2}$ . The surface-cleaned samples of TiFe were subsequently

exposed to increasing doses of  $O_2$ . Further experimental details can be seen elsewhere [12, 14, 18, 29].

The spectra were recorded for the as-inserted samples as well as being registered successively at the end of each sputtering period until all the contamination layers were removed or a steady state was reached. In the case of TiFe samples, spectra were recorded after each dose of  $O_2$  exposure in addition to the as-received and sputtered states. Data were collected either directly on an  $x$ - $y$  recorder using the output of the counter or it was signal averaged, stored and then processed using a microcomputer. The peak positions were assigned by setting the C(1s) contamination signal to a binding energy value of 284.5 eV and  $3d_{5/2}$ -level of silver metal at 368.2 eV. The XPS peaks were deconvoluted according to the procedure described elsewhere [13]. Here we report on the results of the O(1s) region.

## 4. Experimental results

### 4.1. TiFe

XPS and AES studies on TiFe reveal the presence of multiple valence states of both titanium and iron. Although the major portion of titanium is present as  $TiO_2$ , discernible amounts of lower valent oxides, such as  $Ti_2O_3$  and TiO and small amounts of titanium metal are also present in the subsurface [12, 13]. The latter may be a contribution from the alloy itself and not necessarily from pure metal. However, both the possibilities cannot be ruled out. It was also shown that the other component of the alloy, namely iron exists in different oxidation states, such as  $Fe_3O_4$ , FeO and small amounts of iron metal itself, in the subsurface with most of the iron being present as  $Fe_2O_3$  at the outer surface. The same argument for the metallic contribution of iron to that of titanium holds good in this case also. The XPS core level results are further supported by various satellite structures exhibited by the different species [14]. In addition, the X-ray-induced Auger transition (XAES) shows the oxidized nature of iron (KE value, 723.0 eV; LMM region). Similar results were also observed for the activated alloy [12-14, 29]. The spectrum obtained for an  $O_2$ -soaked sample is identical with that of an air-exposed spectrum, indicating that the nature of the species formed on the surface for both the cases is similar in appearance. However, the air-exposed alloy shows slight broadening which may be due to the formation of surface hydroxide and carbonate species. C(1s) [26] and O(1s) results support this observation (see also Table 1).

The Auger spectra of passivated TiFe indicate that the outermost layers are contaminated with carbon and oxygen as revealed by the transitions at 272 eV and 510 eV respectively [15]. The O(KLL) transition, being a measure of the surface  $O_2$  content, shows a marked increase for the activated sample compared with the fresh one [12]. This indicates that the considerable thickness of the surface oxide layers is due to a large segregation of the component elements upon activation. The change in the peak intensities and peak shapes of Auger spectra reveals the influence of the chemical states and composition of the elements [12, 29]. It also



shows that the surface is enriched in iron relative to titanium which has been interpreted on the basis of preferential segregation phenomena (see Section 6). Ion bombardment indicates the presence of various lower valent species [12, 13].

#### 4.2. $LaNi_5$

Core level XPS spectra of the air-exposed sample show that the metal atoms are predominantly in the oxidized state. As expected an enrichment of lanthanum was observed. La(3d) and O(1s) spectra reveal that most of the lanthanum is present as hydroxide,  $La(OH)_3$  whereas the oxide,  $La_2O_3$  is noticed to a lesser extent on the outer surface. Inspection of the C(1s) region suggests that additional  $O_2$  is present on the sample as carbonate, as a small proportion [26]. However, upon sputtering the surface for short periods, the oxide dominates [15, 16]. Since the La(3d<sub>5/2</sub>) region coincides partly with the Ni(2p<sub>3/2</sub>) region it complicates the analysis of the nature of the nickel species besides the low concentration of the metallic component at the surface. Even though the Ni(2p<sub>1/2</sub>) line serves for the identification, the resolution is poor [16] owing to the lower metallic nickel content. However, there are other spectral features that can be useful in identifying the chemical states. For example, the chemical shifts in the XAES lines are usually larger and different from those in the XPS lines and can be measured as accurately as those in the photoelectron lines. This extra information is of significant value. Thus the XAES analysis gave pertinent information regarding the different oxidized species of nickel present on  $LaNi_5$  [15–18]. Further, the results were compared with a similar system, namely  $CaNi_5$  where there is no complication in the Ni(2p<sub>3/2</sub>) region. In addition, various satellites exhibited by the Ni(2p<sub>3/2</sub>) core level also confirm the deductions made from the analysis of the core level spectra and Auger lines. The exact peak positions and the nature of the various species and their assignments based on O(1s) results are summarized in Table 1.

#### 4.3. $CaNi_5$

The Ca(2p) spectra indicate the presence of calcium in the oxidized form, namely as CaO and  $Ca(OH)_2$  [15, 18]. In addition, clear evidence has been shown for the existence of large amounts of carbonate species from C(1s) core level results [26]. It has also been observed that the surface nickel content on  $CaNi_5$  is higher compared with that observed for  $LaNi_5$ . The results were substantiated by the pronounced increase in adsorbed  $CO_2$  on the oxidized nickel surface [26]. Supporting evidence for this observation has been clearly noticed from O(1s) spectra. The peak positions, nature of the surface species and their assignments of different oxygen-containing species that derived from the O(1s) results are listed in Table 1.

#### 4.4. $Mg_2Ni$

The metal core level results show that a surface decomposition and preferential segregation of magnesium on  $Mg_2Ni$  are essentially due to the influence of atmospheric  $O_2$ . Both magnesium and nickel lose their metallic state at the surface completely. The chemical state of the nickel species has been derived from the measured binding energy values of the Ni(2p) lines and from their characteristic

shake-up features. XAES lines give evidence and distinguish the various species clearly [15, 17]. Ion bombardment results in a gradual decrease in the contamination layers and an increase in their metallic content. The O(1s) and C(1s) regions show the existence of both carbonate and hydroxide species of the constituent elements [26]. The various oxidized species deduced from the O(1s) levels are given in Table 1.

#### 4.5. $Mg_2Cu$

It also shows magnesium enrichment on the surface and the segregated magnesium is oxidized upon exposure to air thus exhibiting a similar behaviour to that of  $Mg_2Ni$ . As discussed in the previous section, the formation of various oxides, hydroxides and carbonates are the main products. The energy shift in the Cu( $2p_{3/2}$ ) level suggests the oxidized nature of copper. They are also supported by the prominent satellite features. Upon sputtering, the surface depletes in the oxidized products and a pronounced increase in metallic copper is seen [15, 17]. The different species identified on the surface, based on the O(1s) results, are presented in Table 1. It is known that the oxidation of pure copper metal always leads initially to the formation of  $Cu_2O$  followed by  $CuO$ . Yet the identification of  $Cu_2O$  by XPS alone is quite different owing to the lack of any significant shifts in the 2p-core level emission. Moreover, the chemical state of  $Cu_2O$  cannot be derived from the satellite structures accompanying the  $2p_{3/2}$ -main peak as in  $CuO$ . Therefore another line arising out of XAES transition was used. The change in shape and shifts towards lower kinetic energy of the peak clearly confirm the existence of  $Cu_2O$  along with  $CuO$  and  $Cu(OH)_2$ . Interestingly, the C(1s) shows a pronounced copper concentration on the surface compared with nickel on  $Mg_2Ni$  [26]. This behaviour could be explained on the basis of the surface segregation which will be discussed in the later part of the paper (see Section 6).

#### 4.6. $Mg_2NiH_4$

The air-exposed sample shows features similar to those of  $Mg_2Ni$  and  $Mg_2Cu$ , suggesting the presence of various oxygenated species. However, it is interesting to note that the O(1s) signal is quite broader than that normally observed for the magnesium-based alloys as has been deduced from the FWHM. Typical values are 3.0 eV for  $Mg_2NiH_4$  and about 2.3 eV for both  $Mg_2Ni$  and  $Mg_2Cu$ . This indicates a quite different oxidation behaviour of the hydride surface towards the atmospheric gases. This has been ably supported by C(1s) measurements where it shows more of the basic carbonates than the anhydrous carbonates normally observed with metals and alloys [26]. However, quantitative measurements, as well as detailed studies, are needed to ascertain these findings which in turn give better insight into the chemistry involved in such type reactions.

### 5. Nature of the surface

While extensive studies [2-4, 20, 21, 31, 32] have been reported on the features of bulk properties of  $H_2$  storage materials, not much information is avail-



able on the surface characteristics. The surface studies have received only limited attention [33–36]. The published results on  $\text{LaNi}_5$  reveal some controversy regarding the nature of the species present on the surface. For example, one group [33, 34] have shown an  $\text{O}_2$ -induced segregation of the elements at the surface with the formation of  $\text{La}_2\text{O}_3$  and metallic nickel clusters, whereas the other group [35] have reported that both lanthanum and nickel become oxidized at the surface. However, our own investigations of  $\text{TiFe}$  [12–14],  $\text{Mg}_2\text{Ni}$  [15, 17] and  $\text{Mg}_2\text{Cu}$  [15, 17] as well as of  $\text{LaNi}_5$  [15, 16] and  $\text{CaNi}_5$  [15, 18, 37] demonstrated that the component elements of the alloys are in the oxidized state, resulting in the formation of a variety of oxygenated products, though of different compositions (see Table 1 for a summary of surface analysis data).

In general, the non-oxide species, such as hydroxides and carbonates, on the outer passivated surface have always been considered to be present in small amounts and have been neglected in the past [33, 38]. However, a pronounced increase in hydroxyl species on  $\text{LaNi}_5$  [15, 16] and large amounts of carbonates on  $\text{CaNi}_5$  are noticed [26]. The oxides of lanthanum and calcium are known to adsorb  $\text{H}_2\text{O}$  vapour and  $\text{CO}_2$  quite tenaciously and even when the obvious precautions were taken [39]. It is worthy of note that the presence of various oxide and hydroxide species of lanthanum, calcium and nickel as well as the additional carbonate species on the surface of  $\text{LaNi}_5$  and  $\text{CaNi}_5$  contribute to the broadening of their respective  $\text{O}(1s)$  signals which often complicate the analysis. However, they have been identified clearly with the aid of  $\text{C}(1s)$  signals [26].

In the case of  $\text{TiFe}$ , the presence of compact oxide layers [12–14, 29] prohibits  $\text{H}_2$  absorption. The alloy is deactivated even by exposing it to air for a relatively short time. It requires a special activation procedure to facilitate the  $\text{H}_2$  sorption process, namely treatment of the alloy at high temperatures and high pressures of  $\text{H}_2$  [21]. Although the exact procedure for the activation has been established, the nature and consequences of the activation processes are not fully understood. Many attempts have been made to clarify the mechanism of the sorption process, but no definite understanding has been reached so far [40, 41]. In particular, several models have been proposed with respect to the exact role of the activation process. Changes in activation conditions may lead to preferential precipitation or segregation of the component elements. Surface enrichment of iron rather than titanium was noticed both on unactivated and activated samples. Preferential segregation and oxidation of iron, induced by  $\text{O}_2$  chemisorption and by other factors such as bonding, release of surface strain energy etc., have also been proposed as one of the effects of deactivation of the alloy [12–14, 29].

XPS and AES studies [12–14, 29] revealed the presence of subdioxidic layers of both titanium and iron followed by the formation of higher valent species, namely  $\text{TiO}_2$  and  $\text{Fe}_2\text{O}_3$  respectively on the top. However, the air-exposed samples show considerable broadening of the metal core level peaks of both titanium and iron compared with the  $\text{O}_2$ -exposed samples, suggesting a possible interaction of moisture and atmospheric  $\text{CO}_2$  could be responsible for the observed facts. This has been well supported by the  $\text{C}(1s)$  [26] and  $\text{O}(1s)$  results (Table 1). That is, the formation of hydroxyl and carbonate species alters the metal core levels slightly, thereby causing the damage. It is noteworthy that the carbide layers formed during

sputtering may also alter the metal core level binding energies [30] and this could explain the inconsistencies in the binding energy values often encountered. The O(1s) spectra of the air-exposed and O<sub>2</sub>-exposed samples were dominated by the oxide peaks. However, the spectrum of the air-exposed sample invariably shows shoulders in the high energy region about 1.0 eV apart from the oxide signals of titanium and iron. This could account for the formation of hydroxide species, as it is known that the interaction of TiO<sub>2</sub> and Fe<sub>2</sub>O<sub>3</sub> with H<sub>2</sub>O vapour results in the formation of hydroxyl groups on the surface [42]. However, this feature is completely absent in the case of the O<sub>2</sub>-exposed sample when it is free of moisture and other contaminants.

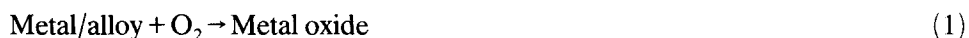
XPS and XAES results for LaNi<sub>5</sub> and CaNi<sub>5</sub> indicate that most of the nickel on the surface is present in the oxidized form, namely NiO, Ni<sub>2</sub>O<sub>3</sub> and Ni(OH)<sub>2</sub> [16, 18, 19]. However, the latter two species are present only on the top layers and hence are considered as saturation or terminal oxide and hydroxide species respectively. Incidentally, these layers are covering the NiO matrix, thus avoiding further diffusion of either O<sub>2</sub> or H<sub>2</sub>O vapour into the bulk thereby protecting the material from further deterioration. In addition, it has been derived from the analyses of Ni(2p<sub>3/2</sub>) and C(1s) regions as well as from Ni(LMM) Auger transitions that there is an enhanced nickel content on the surface of CaNi<sub>5</sub> compared with that of LaNi<sub>5</sub>. Supporting evidence for this observation can be seen from the magnetic susceptibility measurements, which show typical values of  $4.5 \times 10^{-6}$  emu g<sup>-1</sup> and  $6.0 \times 10^{-5}$  emu g<sup>-1</sup> respectively for LaNi<sub>5</sub> and CaNi<sub>5</sub> [43]. The high value for the latter alloy suggests a contribution due to an increase in superparamagnetic nickel particles and this is in accordance with our surface analysis results.

It has been found [44] that the magnesium-based alloys undergo decomposition leading to pronounced enrichment in surface magnesium content, which invariably gets oxidized upon contact with air. In contrast to magnesium, the other alloying elements, namely nickel, copper and indium respectively in Mg-Ni, Mg-Cu and Mg-In alloys have been reported to be metallic even on the air-exposed samples [44, 45]. However, in the case of Mg-Al alloys both magnesium and aluminium are reported to be oxidized at the surface [45]. It has also been suggested that the segregation of magnesium prevents the formation of complete oxide or hydroxide layers of nickel and copper respectively on Mg<sub>2</sub>Ni and Mg<sub>2</sub>Cu by a gettering effect and thereby facilitates the initial adsorption/absorption of H<sub>2</sub> through the underlying clean transition metals [44].

If the above generalization can be made for the magnesium-based alloys, then the so-called activation procedures are not necessary for the initiation and subsequent hydrogen absorption processes. On the contrary, published results on Mg<sub>2</sub>Ni, Mg<sub>2</sub>Cu, and other magnesium-based alloy systems involve a routine activation treatment prior to the formation of the hydrides [20, 46]. Since surface segregation of the components in binary alloy systems is well established, the segregated metal atoms are prone to aerial oxidation and hence the oxidized surface hinders H<sub>2</sub> activation. This could reasonably explain the need for a regular activation treatment that is often practised. This is well supported by our own studies on Mg<sub>2</sub>Ni and Mg<sub>2</sub>Cu [15, 17, 29] which reveal the oxidized nature of the constituent elements of the alloys at the surface. This means that the surface gets activated by

the reduction of the reducible oxidic species and then the  $H_2$  reaction proceeds. The exact nature of the activated species and a possible reaction pathway will be discussed subsequently (see Section 8). It is interesting to note that the relative surface copper present on  $Mg_2Cu$  is higher than that of nickel on  $Mg_2Ni$  as derived from XPS and XAES data and is quite understandable based on their segregation behaviour (see Section 6). It should be pointed out that the oxidation behaviour of the hydride,  $Mg_2NiH_4$  is quite different (even though the products are the same, the product distribution would differ significantly) from the parent alloy [26].

At the outset, it has been deduced that the intermetallic compounds and hydrides examined all decompose at the surface upon contact with air. At the initial stages they combine with  $O_2$  forming their corresponding oxides. Once the oxide layers are formed they, then, react with other gas molecules, such as  $H_2O$  vapour and  $CO_2$  as well as  $O_2$  itself. In other words, a competition among the gas molecules takes place. Since the oxides of most metals are known to react more readily with moisture and  $CO_2$  than  $O_2$  [47], it can be believed that the surface reaction products involve hydroxide and carbonate species. Further  $O_2$  adsorption has little effect, however, producing higher valent or terminal oxides albeit in small amounts. Moisture is observed to adsorb dissociatively, resulting in the formation of hydroxides, whereas  $CO_2$  is found to react associatively to produce different carbonate species. In summary, the overall reactions can be represented in a simple way as



## 6. Surface segregation

Of the various properties of the surface, perhaps, one of the most important that must be known in order to determine any other surface phenomenon is the chemical composition. In many important surface phenomena, such as heterogeneous catalysis, the chemical composition (surface) of the topmost layer controls the properties and not the bulk composition. Often, the active surface is passivated by protective coatings of the various oxidation products. Only recently, through the application of AES, has it been possible to analyse the chemical composition of the first few layers.

Surface segregation is a common feature in most alloys and has been the subject of much theoretical and experimental work [27, 28, 48]. Simple thermodynamic arguments, based on the enthalpy of formation of oxides, can convincingly demonstrate that the surface composition may be very different from the bulk

TABLE 2

Standard enthalpy of oxide formation [55]

<i>Compounds</i>	<i>Heats of formation</i> (kJ mol <sup>-1</sup> )
MgO	-602
CaO	-634
TiO <sub>2</sub>	-944
ZrO <sub>2</sub>	-1104
La <sub>2</sub> O <sub>3</sub>	-1867
Er <sub>2</sub> O <sub>3</sub>	-1899
ThO <sub>2</sub>	-1228
MnO	-385
Fe <sub>2</sub> O <sub>3</sub>	-822
CoO	-239
NiO	-241
CuO	-155

composition for multicomponent systems. In many cases, such simple criteria are sufficient to predict the occurrence of segregation and have good correspondence between them and the experimental results. Nevertheless, these are inadequate for strong, non-ideal metal-metal interactions. In most alloys, it has been reported that the segregating component has a higher O<sub>2</sub> affinity than the other. This is the driving force for segregation involving the differences in the enthalpy of oxide formation. These values for various metal oxides are summarized in Table 2. Accordingly, calcium, zirconium, lanthanum and thorium segregate respectively from CaNi<sub>5</sub>, ZrNi<sub>5</sub>, LaNi<sub>5</sub> and ThNi<sub>5</sub> producing their corresponding oxides at the surface. In the case of TiFe, titanium forms TiO<sub>2</sub>, whereas magnesium results in MgO for both Mg<sub>2</sub>Ni and Mg<sub>2</sub>Cu; erbium forms Er<sub>2</sub>O<sub>3</sub> in the case of ErFe<sub>2</sub>, in accordance with the surface analyses results [12-18, 33-36, 49, 50].

However, there exist some discrepancies and we found that the simple criteria failed for the TiFe alloy. With the advent of AES, it has become possible not only to determine the type of atoms present on the surface, but also to estimate the relative atomic concentrations in the top few layers. The study showed that iron has an enhanced concentration in agreement with a few reports [40, 51]. However, it is quite contrary to quite a few others, where an increase in titanium content was observed [52]. In a similar way, there are some different results for the manganese-based alloys. For example, enrichment of zirconium and titanium were expected, according to the simple segregation conditions, on ZrMn<sub>2</sub> and TiMn<sub>2</sub> respectively. However, XPS investigation on these materials [53] indicated a strange behaviour, namely a preferential segregation and oxidation of manganese atoms. This observation has been explained on the basis of the differences in the surface energies of the components of the alloys. That is, the surface energies favour the segregation of manganese rather than zirconium or titanium in agreement with the experimental results. Accordingly, in multicomponent systems, the element which

TABLE 3

Some properties of a few selected elements [28, 55]

<i>Element</i>	<i>Atomic radius</i> (Å)	<i>Surface energy</i> (mJ m <sup>-2</sup> )	<i>Latent heat of vapourization</i> <sup>a</sup> (kJ mol <sup>-1</sup> )	<i>Latent heat of sublimation</i> <sup>b</sup> (kJ mol <sup>-1</sup> )	<i>E</i> <sup>c</sup> (kJ mol <sup>-1</sup> )
Mg	1.72	790	128	147	—
Ca	2.23	490	151	176	—
Ti	2.00	2050	426	469	555
Zr	2.16	1950	580	612	635
La	2.74	900	402	423	405
Mn	1.79	1600	231	291	355
Fe	1.72	2550	340	399	535
Co	1.67	2550	—	425	505
Ni	1.62	2450	374	430	485
Cu	1.57	1850	304	341	385

<sup>a</sup>At room temperature.<sup>b</sup>At boiling point.<sup>c</sup>A parameter which is related to surface energy and heat of vapourization [28].

has a lower surface energy will preferentially segregate to the surface, even before contacting with O<sub>2</sub> or air. However, in the case of alloys, such as CaNi<sub>5</sub>, ZrNi<sub>5</sub>, LaNi<sub>5</sub>, ThNi<sub>5</sub>, Mg<sub>2</sub>Ni, Mg<sub>2</sub>Cu, or ErFe<sub>2</sub> whether we use the differences in the surface energies or the differences in the enthalpy of formation of oxides, it will lead to similar predictions for the segregation effects. The surface energies of various metals are given in Table 3.

In the case of AB<sub>5</sub>-systems, besides the concentration of A-atoms, the relative amount of B-atoms also seem to be different and vary for various A- and B-combinations. For example, for a system such as CaNi<sub>5</sub>, we observed an increase in nickel concentration relative to that for LaNi<sub>5</sub>. This could again be attributed to various segregation parameters that are listed in Tables 2 and 3. In particular, the enthalpy of oxide formation for CaO is lower compared with La<sub>2</sub>O<sub>3</sub>, thereby the relative concentration of CaO is expected to be low on CaNi<sub>5</sub> compared with that of La<sub>2</sub>O<sub>3</sub> on LaNi<sub>5</sub>. As a consequence, we would expect a larger nickel concentration on CaNi<sub>5</sub>. This gives a clue for the experimentally observed enhanced amounts of nickel on CaNi<sub>5</sub>. In a similar way, the enrichment of nickel on ZrNi<sub>5</sub> compared with ThNi<sub>5</sub> [49] can be explained.

Based on the experimental results and the foregoing arguments, the concentration of nickel on the air-exposed samples of various alloys at room temperature can be arranged in the following order:

$$\text{CaNi}_5 > \text{ZrNi}_5 > \text{ThNi}_5 > \text{LaNi}_5 \quad (7)$$

However, the sequence might vary under different experimental conditions, such as for varying pressures and temperatures employed for the activation treatment.

The increase in nickel content on the surface of the  $\text{CaNi}_5$  alloy clearly indicates the ease of activation of this alloy compared with  $\text{LaNi}_5$ . Moreover, the enhanced nickel concentration will play an important role in the catalytic properties, such as in hydrogenation reactions.

However, the  $\text{A}_2\text{B}$ -system shows enrichment of A-atoms on the surface in accordance with the arguments based on segregation criteria as well as from experimental results. For example,  $\text{Mg}_2\text{Ni}$  and  $\text{Mg}_2\text{Cu}$  show enrichment of magnesium at the surface. However, there is a difference in the relative amounts of the transition elements in each case. That is, the concentrations of nickel and copper are quite different. XPS results indicate clearly the presence of more copper on  $\text{Mg}_2\text{Cu}$  than of nickel on  $\text{Mg}_2\text{Ni}$  [17, 26]. This is quite understandable by considering the different segregation parameters given in Tables 2 and 3. Hence, in this case also the activation treatment and the catalytic properties, if any, might be expected to vary.

AES investigations on  $\text{TiFe}$  (AB-system) show the preferential segregation of iron rather than titanium, unlike, as predicted by enthalpy and surface energy considerations (Tables 2 and 3) as well as from the experimental results [52]. Therefore it can be deduced that some other parameters, in addition to the thermodynamic and surface energy factors, may be responsible for the observed segregation in  $\text{TiFe}$ . Different energy terms have been considered for this purpose and it is deduced that the driving force for the observed segregation could be due to the differences in surface energy and/or heat of vapourization or sublimation of the components of the alloy. These factors can be of importance in specific cases, such as  $\text{TiFe}$ . Therefore segregation is considered to be associated with a number of other parameters, namely bond strength, atomic size, surface tension etc., and subsequently expected to have an influence on the surface concentration of the components. In addition, some other factors, such as entropy effects, elastic size mismatch energy, release of bulk strain energy etc., [28] can also contribute in selected systems, though only to a limited extent. Thus the enrichment of iron overlayers on  $\text{TiFe}$  alloy can be explained by the segregation parameters, namely the heat of vapourization and sublimation or by a parameter " $E$ " (see Table 3) which is related to the surface energy and heat of vapourization [28]. The differences in these values can account for the experimentally observed segregation. These values for iron are lower than that for titanium and hence favour the segregation of iron followed by titanium. That is, the segregation would have taken place well ahead of the  $\text{O}_2$ -induced process.

## 7. Oxidation behaviour

The initial hydriding reaction of the alloys is mainly controlled by the transition metal present on the surface. Clearly, a knowledge of their oxidation and reduction behaviours, and their dependences under different atmospheres (reactive gases) are of importance in order to understand the various surface processes, as they play a key role in the hydriding and dehydriding mechanisms. For example, the initial hydriding of  $\text{LaNi}_5$  and  $\text{CaNi}_5$  is quite easy compared with

many other alloys, mainly because of their very different segregation and oxidation behaviours. Although the oxidation of metal surfaces is a very common feature, it is poorly understood. The reason for this is that the actual oxidation process of a metal involves several complicated steps, in particular the transition metals which are known to exhibit different oxidation states. It could be described as follows: as a primary step, the  $O_2$  molecules must adsorb and dissociate into atoms they then have to diffuse through an initial oxide layer and finally react with the underlying metal. These processes often occur at ambient (pressure and temperature) conditions of  $O_2$ . In addition to  $O_2$ , moisture and atmospheric  $CO_2$  can also react with the metal and/or the oxidized surface thereby complicating the process further. In order to understand why some of the transition metals show good resistance to oxidation while others do not, it will be of use to consider the energy barrier to  $O_2$  penetration on the metal and oxide surfaces—a measure of oxidation resistance [54].

In particular, the formation of NiO on a nickel surface dramatically increases the potential barrier for  $O_2$  incorporation. However, on copper the formation of an oxide layer reduces the barrier. Whereas for titanium and iron the barriers on the metals and on their respective oxides are similar (see Table 4). Accordingly, nickel-containing alloys, such as  $LaNi_5$ ,  $CaNi_5$ ,  $Mg_2Ni$  etc., are expected to form a thin oxide layer of nickel and others, such as  $TiFe$  and  $Mg_2Cu$  of iron and copper respectively, are believed to form much thicker oxide coatings. These predictions are in close agreement with the surface analytical results. This accounts for the different activation procedure required for the various alloys.

It was shown that the magnitude of the barrier depends on both the structure and the ability of the surface atoms to relax during the incorporation process. The

TABLE 4

Parameters which influence the oxygen penetration of materials [54]

<i>Materials</i>	<i>Unrelaxed barrier (eV)<sup>a</sup></i>	<i>Relaxed barrier (eV)<sup>a</sup></i>
Ti	0.26	0.18
Mn	2.70	0.85
Fe	2.87	1.46
Co	4.22	1.74
Ni	4.12	1.69
Cu	2.80	0.88
$TiO_2$	0.16	0.07
MnO	2.58	0.97
$Fe_3O_4^b$	0.49	0.21
CoO	4.62	1.51
NiO	5.58	1.79
$Cu_2O$	0.16	0.03

<sup>a</sup>The magnitude of the barrier depends on both the structure and the ability of the surface atoms to relax (elastic property) during the incorporation process.

<sup>b</sup>Since  $Fe_2O_3$  can be considered as a spinel structure with vacant positions in the metal lattice and for the simplicity in the calculation  $Fe_3O_4$  has been used.

energy barriers for  $O_2$  on a transition metal oxide surface can be very different from the barrier on the corresponding clean metal surface. This has an important consequence, in that a metal's resistance to oxidation can be improved dramatically by the formation of an oxide layer (a well-known fact also). The barrier for  $O_2$  penetration very much depends on the structure and the stoichiometry of the oxide (Table 4). As has been mentioned earlier, the type of element at the surface of the alloys plays an absolutely crucial role in protecting the material from further deterioration. This is best exemplified by a comparison of the energy barrier for oxides of transition metals which form a variety of structures [54]. It is to be noted that defects in the oxide structures can open up diffusion paths with much lower activation energies than the perfect structures.

## 8. Activation model

To date, a number of suggestions have been made concerning the mechanism which controls the transfer of hydrogen from surface to bulk. For example, in the case of a well-studied system, such as TiFe, various processes, namely surface segregation and catalysis, oxide cracking, oxide layer dissolution, permeability of surface oxide layers etc., have been suggested for the hydrogen reaction [56]. Still, a complete understanding of the changes involved during the initial activation and cyclic deactivation processes is unclear. Some controversies exist about the fundamental aspects of the sorption behaviour, such as the role of surface composition, activation mechanism, stability and the nature of different species present on the surface. Hence the surface chemistry and structure of the poisoned material are not yet fully understood. In particular, the formation of hydrides of TiFe is inhibited by the surface deactivation through the presence of protective oxide layers ( $TiO_2$  and  $Fe_2O_3$ ). These layers become inactive owing to impeded hydrogen ( $H_2$ ) dissociation on the oxide surface or slow hydrogen (H) permeation through the protective layers and hence the kinetics of hydrogen (H) sorption are considerably affected as also the storage capacity. It is well known that the clean surfaces of many transition metals are able to adsorb  $H_2$  dissociatively and desorb it associatively [57]. Hence, the 3d elements play an important role in the initial  $H_2$  sorption processes. Unlike the TiFe alloys, the nickel-based systems (e.g.  $CaNi_5$ ,  $ZrNi_5$ ,  $ThNi_5$ ,  $LaNi_5$ ,  $Mg_2Ni$  and  $ZrNi_2$ ) can be activated without much difficulty. NiO formed on the surface can be easily reduced by  $H_2$  (even at room temperature) to produce active nickel clusters [9, 58], whereas the reduction of the oxide ( $Fe_2O_3$ ) produced on TiFe surface under these conditions is rather difficult.

A number of studies [59] have been reported on the reduction of iron oxides. It follows a stepwise process and the complete reduction (iron oxide to iron metal) takes place only above  $570^\circ C$ . It also depends on various parameters, such as the reduction temperature,  $H_2O$  vapour partial pressure, particles size etc. In addition, the inherent presence of  $TiO_2$  would further increase the reduction temperature [60]. Therefore the reduction of the surface oxides of TiFe is difficult and hence cannot produce active sites under normal activation conditions employed for the nickel-based alloys. This accounts for the special activation procedure that is



normally employed for TiFe alloy. Even though a general agreement has been reached in recognizing the important role of  $O_2$  in TiFe activation and deactivation processes, the actual mechanism of the reaction and the role of various reactant products at the surface is diffuse. Since, the surface free energy is large for metals, and the interaction between metal and substrate is relatively weak, metal crystallites will not spread over the surface of the oxide substrate, when the alloy is activated either in vacuum or in a hydrogen atmosphere. Whereas, in an  $O_2$  atmosphere, the metal is oxidized and as a result, the surface free energy becomes much smaller than that of the metal. The interactions between the oxidized metal and the oxide substrate are also stronger than those between metal and substrate. However, only if they are sufficiently strong can the oxidized metal spread over the substrate.

Recently, we proposed [19] an activation model for  $LaNi_5$  and  $CaNi_5$  for  $H_2$  uptake. According to this model, the surface oxides produced on these alloys may behave like metal-supported systems (for example,  $Ni/La_2O_3$  and  $Ni/CaO$  in the cases of  $LaNi_5$  and  $CaNi_5$  respectively), which are known to possess higher catalytic activity towards  $H_2$ . Based on this model, the easy activation and rapid kinetics of these systems have been explained. As pointed out above, a similar mechanism could also be extended for the other systems. Previous investigations [41, 52] on the activation of TiFe have resulted in two conflicting models regarding the initial activation of  $H_2$  molecule. One model demonstrates that the initial activation involves the formation of metallic iron clusters and  $TiO_2$  on the surface. The metallic iron clusters dissociate  $H_2$  molecules and incorporate into the bulk. The second model suggests that the formation of a ternary oxide is responsible for the initial activation of  $H_2$ . In this account, earlier, we have presented some significant surface property-activation and deactivation relations for TiFe. Accordingly, the precipitated or segregated iron islands on the surface (possibly in the oxidized form) can be embedded in the underlying  $TiO_2$  matrix. Upon activation, the surface may typically function like a typical metal support system, namely  $Fe/TiO_2$ . Therefore it is possible to state that, in general, the intermetallic compounds decompose on the surface resulting in the formation of numerous oxidized species and a uniform distribution of the products. Upon activation, the surface typically functions like a supported metal system, namely  $Ni/La_2O_3$ ,  $Ni/CaO$ ,  $Ni/MgO$ ,  $Cu/MgO$  and  $Fe/TiO_2$  respectively on  $LaNi_5$ ,  $CaNi_5$ ,  $Mg_2Ni$ ,  $Mg_2Cu$  and TiFe. Since the supported metal systems are known to exhibit good chemisorption properties they hence would account for the observed sorption behaviour of the alloys.

## 9. Conclusion

The initial stages of decomposition of the intermetallic compounds result in the formation of oxides of the constituent elements upon exposure to atmosphere. Since the oxides are known to react readily with moisture and  $CO_2$ , they produce hydroxides and carbonates respectively. These species are to be expected by considering their chemical reactivity and hence are present to a considerable extent on the surface of these alloys. The interaction of  $O_2$  also results in the formation of

terminal or higher valent oxides in certain cases. Therefore the activation procedures developed for these alloys should take into account the relative amounts of different species at the surface and at times the attendant preferential segregation of one of the constituents of the alloy. The chemical-reaction-induced segregation may be the main factor which is contributing to the difference in the surface concentration of the various species. However, other segregation parameters could also equally play important roles in specific cases, such as TiFe where an enhanced concentration of iron instead of titanium was observed.

It is interesting to note that the systems under investigation behave differently among themselves with respect to the surface oxidation and the surface composition of the various species on the top few layers are quite different. For example,  $\text{LaNi}_5$  shows large amounts of hydroxyl species [15, 16, 19, 26], and carbonates [15, 18, 19, 26] seem to be predominant in the case of  $\text{CaNi}_5$ , whereas the alloys,  $\text{Mg}_2\text{Ni}$  and  $\text{Mg}_2\text{Cu}$ , and the hydride,  $\text{Mg}_2\text{NiH}_4$  indicate a distribution of both hydroxyl and carbonate species nearly equally [15, 17, 22, 26], but an enhanced concentration of oxides rather than hydroxides or carbonates is observed on TiFe [12–14, 26]. This is mainly because of the quite different segregation nature of the alloys and hydrides, and the specific reactivity of the segregated metals towards various gas molecules. All these compounds (oxides, hydroxides and carbonates) are likely surface oxidation products of the alloys and hydrides and their chemical differentiation from the substrate is thus important. In general, the hydroxide and/or carbonate species persist only on the outer passivated (oxidic) surface.

The gradual loss in  $\text{H}_2$  sorption capacity of materials after a number of charge–discharge cycles could be accounted for in the decomposition of the alloys in terms of the reaction with trace levels of  $\text{O}_2$  and/or  $\text{H}_2\text{O}$  vapour present in the feed  $\text{H}_2$  gas. Each of the oxidation products is relatively inactive toward  $\text{H}_2$  sorption and they periodically accumulate over a number of absorption–desorption cycles. Thus a drastic loss in the storage capacity is experienced besides deactivation of the alloys. However, the fast reaction kinetics of the intermetallic compounds, after an initial activation process, could be explained based on the supported metal system exhibited on the surface. That is, the active metal is expected to disperse uniformly on the support matrix which is known to have better hydrogenation kinetics. This explains the rapid uptake of hydrogen for the activated samples. The easy activation of nickel-containing samples, such as  $\text{LaNi}_5$ ,  $\text{CaNi}_5$  and  $\text{Mg}_2\text{Ni}$  could be due to the easy reducibility and the oxidation resistance of the NiO present at the surface contrary to the TiFe where an opposite trend has been noticed. In addition, the very excess nickel content of the alloys accounts for the excellent/high reaction rates of  $\text{LaNi}_5$  and  $\text{CaNi}_5$ .

### Acknowledgments

Our thanks to Professor K. Yvon, University of Geneva for his continued support. We are grateful to RSIC, IIT, Madras for the ESCA and AES measurements.

## References

- 1 P. Selvam, B. Viswanathan and V. Srinivasan, *20th Natl. Seminar on Effective Energy Management, Steam and Fuel Users' Association of India, Madras, December 4-6, 1987*, p. G1 and references cited therein.
- 2 See for example: G. G. Libowitz, *The Solid State Chemistry of Binary Hydrides*, Benjamin, New York, 1965; W. M. Mueller, J. P. Blackledge and G. G. Libowitz (eds.), *Metal Hydrides*, Academic Press, New York, 1968; G. Alefeld and J. Volkl (eds.), *Hydrogen in Metals I & II, Topics in Applied Physics*, Vols. 28, 29, Springer, Heidelberg, 1978; L. Schlapbach (ed.), *Hydrogen in Intermetallic Compounds I, Topics in Applied Physics*, Vol. 63, Springer, Heidelberg, 1988.
- 3 P. Selvam, B. Viswanathan, C. S. Swamy and V. Srinivasan, *Int. J. Hydrogen Energy*, *11* (1986) 169; and references cited therein.
- 4 J. H. N. van Vucht, F. A. Kuijpers and H. C. A. M. Burning, *Philips Res. Rep.*, *25* (1970) 133; H. H. van Mal, K. H. J. Buschow and A. R. Miedema, *J. Less-Common Met.*, *35* (1974) 65.
- 5 H. Buchner, *Prog. Energy Combust. Sci.*, *6* (1980) 331.
- 6 G. D. Sandrock and P. D. Goodell, *J. Less-Common Met.*, *104* (1984) 159.
- 7 H. Uchida and M. Ozawa, *Z. Phys. Chem. N.F.*, *147* (1986) 77.
- 8 J. Genossar and P. S. Rudman, *Z. Phys. Chem. N.F.*, *116* (1979) 215.
- 9 N. Birks and G. H. Meier, *Introduction to High Temperature Oxidation of Metals*, Arnold, London, 1983.
- 10 H. G. Wulz and E. Fromm, *J. Less-Common Met.*, *118* (1986) 293, 315.
- 11 E. Fromm, *Z. Phys. Chem. N.F.*, *147* (1986) 61.
- 12 P. Selvam, B. Viswanathan, C. S. Swamy and V. Srinivasan, in S. R. Naidu and B. K. Banerjee (eds.), *Proc. 8th Natl. Symp. on Challenges in Catalysis—Science and Technology, PDIL, Sindri, February 12-14, 1987*, p. 306.
- 13 P. Selvam, B. Viswanathan, C. S. Swamy and V. Srinivasan, *Int. J. Hydrogen Energy*, *12* (1987) 245.
- 14 P. Selvam, B. Viswanathan, C. S. Swamy and V. Srinivasan, *Indian J. Technol.*, *25* (1987) 639.
- 15 P. Selvam, B. Viswanathan, C. S. Swamy and V. Srinivasan, *Z. Phys. Chem. N.F.*, *164* (1989) 1199.
- 16 P. Selvam, B. Viswanathan, C. S. Swamy and V. Srinivasan, submitted to *Int. J. Hydrogen Energy*.
- 17 P. Selvam, B. Viswanathan and V. Srinivasan, *Int. J. Hydrogen Energy*, *14* (1989) 899.
- 18 P. Selvam, B. Viswanathan and V. Srinivasan, *J. Electron Spectrosc. Relat. Phenom.*, *49* (1989) 203.
- 19 P. Selvam, B. Viswanathan and V. Srinivasan, *Int. J. Hydrogen Energy*, *14* (1989) 687.
- 20 J. J. Reilly and R. J. Wiswall, Jr., *Inorg. Chem.*, *6* (1967) 2220; *7* (1968) 2254.
- 21 J. J. Reilly and R. H. Wiswall, Jr., *Inorg. Chem.*, *13* (1974) 218.
- 22 P. Selvam, B. Viswanathan and V. Srinivasan, *J. Electron Spectrosc. Relat. Phenom.*, *46* (1988) 357.
- 23 P. Selvam, B. Viswanathan, C. S. Swamy and V. Srinivasan, *Bull. Mater. Sci.*, *9* (1987) 21; *Thermochim. Acta*, *125* (1988) 1; *Int. J. Hydrogen Energy*, *13* (1988) 87, 749.
- 24 S. Ono, Y. Ishido and J. Kitagawa, *Proc. JIMIS-2, Hydrogen in Metals, 1980*, p. 357.
- 25 D. M. Gualtieri, K. S. V. L. Narasimhan and T. Takeshita, *J. Appl. Phys.*, *47* (1976) 3432.
- 26 P. Selvam, B. Viswanathan and V. Srinivasan, *Int. J. Hydrogen Energy*, *15* (1990) 133; *J. Less-Common Met.*, *158* (1990) L1.
- 27 S. H. Overburg, P. A. Bertrand and G. A. Somorjai, *Chem. Rev.*, *75* (1975) 547; M. S. Spencer, *Surf. Sci.*, *145* (1984) 145, 153; F. F. Abraham and C. R. Brundle, *J. Vac. Sci. Technol.*, *18* (1981) 506.
- 28 A. R. Miedema, *Z. Metallkd.*, *69* (1978) 455.
- 29 P. Selvam, *Ph.D. Thesis*, Indian Institute of Technology, Madras, 1987.
- 30 P. Selvam, B. Viswanathan and V. Srinivasan, *J. Less-Common Met.*, *161* (1990) in the press; *J. Electron Spectrosc. Relat. Phenom.*, (1990) in the press.
- 31 H. H. van Mal, *Philips Res. Rep.*, Suppl. No. 1 (1976).
- 32 P. Fischer, A. Furrer, G. Busch and L. Schlapbach, *Helv. Phys. Acta*, *50* (1977) 421; A. Yoshikawa and T. Matsumoto, *J. Less-Common Met.*, *84* (1982) 263.
- 33 H. C. Siegmann, L. Schlapbach and C. R. Brundle, *Phys. Rev. Lett.*, *40* (1978) 972.
- 34 Th. von Waldkirch and P. Zurcher, *Appl. Phys. Lett.*, *33* (1978) 689; L. Schlapbach, *Solid State Commun.*, *38* (1981) 117.

- 35 W. E. Wallace, R. F. Karlicek and H. Imamura, *J. Phys. Chem.*, **83** (1979) 1708; J. H. Weaver, A. Franciosi, W. E. Wallace and H. K. Smith, *J. Appl. Phys.*, **51** (1980) 5847; J. H. Weaver, A. Franciosi, D. J. Petermaen, T. Takeshita and K. A. Gschneidner, *J. Less-Common Met.*, **86** (1982) 195.
- 36 N. Shamir, U. Atzmony, Z. Gavra and M. H. Mintz, *J. Less-Common Met.*, **103** (1984) 367.
- 37 M. P. Sridharkumar, B. Viswanathan, C. S. Swamy and V. Srinivasan, *J. Mater. Sci.*, **21** (1986) 2335.
- 38 T. L. Barr, *J. Phys. Chem.*, **82** (1978) 1801.
- 39 See for example: P. Buoroughts, A. Hammett, A. F. Orchard and G. Thorton, *J. Chem. Soc. Dalton Trans.*, **17** (1976) 1686; C. K. Jorgensen and H. Berthon, *Chem. Phys. Lett.*, **13** (1972) 186; S. Myhra, H. E. Bishop, J. C. Riviere and M. Stephenson, *J. Mater. Sci.*, **22** (1987) 3217.
- 40 L. Schlapbach and T. Riesterer, *Appl. Phys.*, **A32** (1983) 169; and references cited therein.
- 41 H. Zuchner, U. Bilitceski and G. Kirch, *J. Less-Common Met.*, **101** (1984) 441.
- 42 See for example: C. N. Sayers and N. R. Armstrong, *Surf. Sci.*, **77** (1978) 301; G. C. Allen, P. M. Tucker and R. K. Wild, *Philos. Mag.*, **46B** (1982) 411; P. Mills and J. L. Sullivan, *J. Phys. D.*, **16** (1983) 723; S. Bourgeois, C. Gimenz and M. Perdereau, in P. Barret and L. C. Dufour (eds.), *Proc. 10th Int. Symp. on the Reactivity of Solids, August 27-31, 1984*.
- 43 L. Schlapbach, F. Stucki, A. Seiler and H. C. Siegmann, *J. Magn. Magn. Mater.*, **15-18** (1980) 1271; K. Yagisawa and A. Yoshikawa, *Z. Phys. Chem. N.F.*, **117** (1979) 79.
- 44 A. Seiler, L. Schlapbach, Th. von Waldkirch, D. Shaltiel and F. Stucki, *J. Less-Common Met.*, **73** (1980) 193.
- 45 N. Shamir, M. H. Mintz, J. Bloch and V. Atzmony, *J. Less-Common Met.*, **92** (1983) 253.
- 46 See for example: Ph. Guinet, P. Perroud and J. Reblers, in T. N. Veziroglu and W. Seifritz (eds.), *Proc. 2nd World Hydrogen Energy Conf., Zurich, August 21-24, 1978*, Vol. 3, Pergamon, New York, 1978, p. 1657; H. Buchner, O. Bernauer and W. Straub, in T. N. Veziroglu and W. Seifritz (eds.), *Proc. 2nd World Hydrogen Energy Conf., Zurich, August 21-24, 1978*, p. 1677. M. H. Mintz, S. Malkieley, Z. Gavra and Z. Hadari, *J. Inorg. Nucl. Chem.*, **40** (1978) 1949; G. Bruzzone, G. Costa, M. Ferritti and G. L. Olcese, *Int. J. Hydrogen Energy*, **8** (1983) 459; V. N. Verbetskii, A. N. Sytnikov and K. N. Semenenko, *Russ. J. Inorg. Chem.*, **29** (1984) 360.
- 47 F. A. Cotton and G. Wilkinson, *Advanced Inorganic Chemistry*, Wiley, New York, 1972.
- 48 M. P. Seah, in D. Briggs and M. P. Seah (eds.), *Practical Surface Analysis by Auger and X-ray Photoelectron Spectroscopy*, Wiley, Chichester, 1983.
- 49 A. G. Moldovan, E. Elattar and W. E. Wallace, *J. Solid State Chem.*, **25** (1978) 23.
- 50 L. Schlapbach and C. R. Brundle, *J. Phys.*, **42** (1981) 1025; A. Seiler, L. Schlapbach and H. Scherrer, *Surf. Sci.*, **121** (1982) 98.
- 51 H. Zuchner and G. Kirch, *J. Less-Common Met.*, **101** (1984) 441.
- 52 L. Schlapbach, A. Seiler and F. Stucki, *Mater. Res. Bull.*, **13** (1978) 1031; L. Schlapbach, A. Seiler, F. Stucki, P. Zurcher, P. Fischer and J. Schefer, *Z. Phys. Chem. N.F.*, **117** (1979) 54, 205; M. Polak and Y. Ben-Shoshan, *Surf. Sci.*, **146** (1984) L601.
- 53 L. Schlapbach, *J. Less-Common Met.*, **89** (1983) 37.
- 54 P. Nordlander and M. Ronay, *Phys. Rev. B*, **36** (1987) 4982.
- 55 *Smithells Metals Reference Book*, Butterworths, London, 6th edn., 1983; *CRC Handbook of Chemistry and Physics*, CRC Press, Boca Raton, FL, 64th edn., 1983-1984.
- 56 F. D. Manchester and D. Khatamian, in R. G. Branes (ed.), *Hydrogen Storage Materials*, Mater. Sci. Forum **31** (1988) 261; and references cited therein.
- 57 G. C. Bond, *Catalysis by Metals*, Academic Press, New York, 1962.
- 58 D. R. Gaskell, *Introduction to Metallurgical Thermodynamics*, McGraw-Hill, Kokakusha, 1973.
- 59 See for example: M. Shimokawaba, R. Furuichi and T. Ishii, *Thermochim. Acta*, **28** (1979) 287; O. J. Wimmers, P. Arnoldy and J. A. Moulijn, *J. Phys. Chem.*, **90** (1986) 1331; M. V. C. Sastri, R. P. Viswanath and B. Viswanathan, *Int. J. Hydrogen Energy*, **12** (1982) 951.
- 60 M. Shimokawava, R. Furuichi and T. Ishii, *Thermochim. Acta*, **28** (1979) 287.